

A novel simple GMPPT method based on probability distribution of global maximum power point under partial shading conditions

K.B.K. Cao¹ and V. Boitier²

¹ Department of Energy and Embedded Systems
LAAS-CNRS, Université de Toulouse, CNRS
7 Av. Du Colonel Roche, 31400 Toulouse (France)
Email: kha-bao-khan.cao@laas.fr

² Department of Energy and Embedded Systems
LAAS-CNRS, Université de Toulouse, CNRS
7 Av. Du Colonel Roche, 31400 Toulouse (France)
Email: vboitier@laas.fr

Abstract.

A photovoltaic (PV) array having multiple cells in series with bypass diodes may exhibit multiple power peaks under uneven irradiation, therefore an algorithm is required to reach the global maximum power point (GMPP). While a lot of methods have been proposed in the literature, they are usually quite complex and does not fully utilize the characteristics of the PV array. This paper first highlights a rapid and optimized mathematical simulation of the PV array using MATLAB to find the probability distribution of voltage at GMPP under multiple irradiation conditions and temperatures. The resulting GMPP distribution in 22E6 irradiation and temperature conditions checked for an array of 4 PV modules in series with bypass diodes is presented, as well as the optimizations in MATLAB necessary to keep simulation time in check. From the obtained result, we propose a simple and efficient probability-based algorithm capable of reaching GMPP up to 93.64% of the time.

Key words. Global maximum power point tracking algorithm (GMPPT), partial shading, Lambert W function, probability distribution, MATLAB/Simulink

1. Introduction

Harvesting energy through PV is usually the simplest and most viable source for mobile embedded systems away from the grid. Some examples are remote sensors to monitor a jungle's ecosystem and a mountaineer up in the Alps trying to charge his/her phone. This mobility and unstable operating conditions mean that such PV systems must be efficient, resilient against rapidly changing irradiation and partial shading, yet simple enough to be put on a low power microcontroller (μ C) (e.g., PIC18 8-bit μ C family) Since PV cells are connected in series to increase harvesting potential, uneven insolation across the array may cause hotspots that accelerate degradation as well as significantly reduce the array's power output [1]. Therefore, bypass diodes are usually used to provide a current path around the shaded modules, but this leads to multiple power peaks at the detriment of control efficiency (Figure 1) [2], [3].

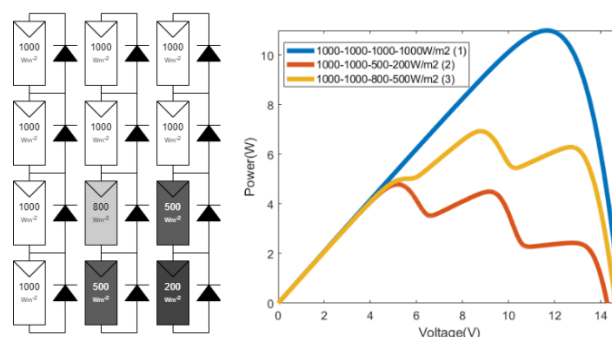


Figure 1 Power output of 4 PV modules in series with bypass diodes under different irradiation conditions

Considering that under perfect irradiation the PV array still has a maximum power peak, there are great interest in optimizing PV systems in the literature which can be classified into 2 categories of algorithms: single peak capable and multiple peaks capable. The most well-known amongst the former are Perturb and Observe (P&O) [4], Incremental Conductance (IC) [5], β -parameter method [6], fractional open circuit voltage (V_{oc}) [7], MPP locus characterization [8] and temperature based approximation of MPP [9]. In general, these algorithms are simple to implement and are efficient under good and stable weather conditions, but they cannot guarantee optimal power acquisition in less-than-ideal conditions. The multiple peaks capable methods on the other hand are capable of identify the true MPP when the array is partially shaded, and they can be divided into several sub-classes of algorithms. The first are improved versions of single peak capable methods like improved P&O or incremental conductance with zoning to multiples of $0.8V_{oc}$ [10]–[13], which take advantage of the fact that the MPP of a single module can be found in this region. These approaches are also simple and decently good under stable weather conditions, but they fail to consider the voltage drop caused by activated bypass diodes and their convergence times are not great. The second type of GMPP methods are optimization algorithm based like genetic algorithm [14], differential evolution [15], particle swarm optimization (PSO) [16], [17], artificial bee colony (ABC) [18],

grasshopper optimization [19], grey-wolf optimization (GWO) [20]–[22], flower pollination algorithm [23], student psychology based optimization [24], dragonfly algorithm [25], ant colony optimization [26], Henry gas solubility optimization [27] and cuckoo search algorithm [28]. These approaches can identify GMPP, but they suffer from several drawbacks, most notably their implementation complexity (e.g., floating points operations, exponentials, logarithms) and wild power swings during the search phase. Finally, there are fuzzy logic controllers methods [29]–[31] and neural network MPPT [32], which are all too heavy on a low-power μ C. Another problem missing in the current literature was the distribution of GMPP for a particular PV installation. Currently, our models for PV arrays are quite precise with the simple single diode model [33]–[35] and Simulink has proven to be an effective simulation tool for PV applications [36]. Moreover, there exists a computational method based on the Lambert W function that would vastly reduce the time needed to solve the PV equation [37]–[39]. However, most of the efforts to solve the PV equation mainly focus on obtaining the current output of a single PV module without any bypass diode and there was not yet any proposition on how to efficiently build the current output profile of an entire array with multiple bypass diodes numerically besides using Simulink. This method is acceptable if we are to perform a few simulations, but to observe the array's performance under a wider range of weather conditions, it quickly becomes inefficient (i.e., 375000 conditions simulation take 8h45min using MATLAB/Simulink 2020b on 8 parallel threads using a Ryzen 7 3700X 8-cores processor, 32GB of DDR4 3200MT/s).

In this paper, we propose an optimized method to simulate the power output of a PV array and help to visualize the distribution of GMPP under a very wide range of irradiation and weather conditions. From this result, we will also be proposing a probabilistic approach to improve the traditional P&O method that should have a fast convergence time as well as simple enough to be easily implemented on a low power μ C. The preliminary proof-of-concept will be done in simulation via Simulink and compared to deterministic PSO, GWO and ABC algorithms. All results presented were tested using 4 PV monocrystalline modules in series with bypass diodes whose characteristics will be detailed in the later sections (Figure 2).

2. Modelling PV arrays with bypass diodes under partial shading

Since each one of our PV modules consist of 6 smaller cells in series, its model can be obtained via the modified single diode model as shown in Figure 3 and from the work of [34], we obtain the mathematical equations modelling our PV modules (1).

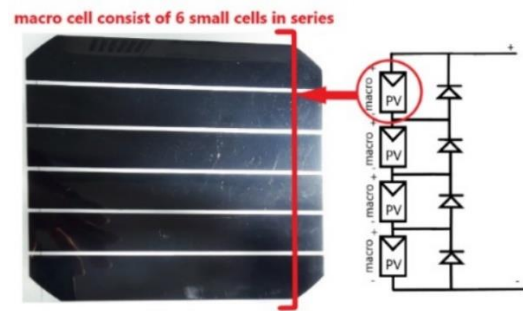


Figure 2 PV modules whose parameters were used for the simulations

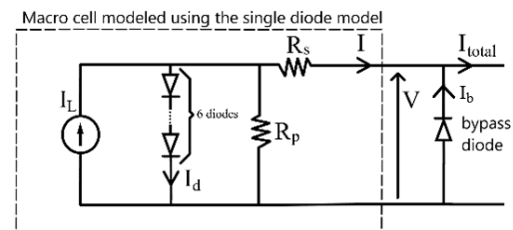


Figure 3 Single diode model of the PV module and its respective bypass diode

$$I = I_L - I_d - \frac{V + IR_s}{R_p} \quad (1)$$

$$I_L = \frac{G}{G_{ref}} (I_{scn} (1 + \frac{R_s}{R_p}) + k_i(T - T_{ref}))$$

$$I_d = I_0 (e^{\frac{q}{AKT}(V + IR_s)} - 1)$$

$$I_0 = \frac{I_{scn} + k_i(T - T_{ref})}{e^{\frac{q}{AKT}(V_{ocn} + k_v(T - T_{ref}))} - 1}$$

Solving the methods proposed in [39], we obtain the explicit expression of current I for a given V, G and T (2).

$$I = X - \frac{\text{Lambert}(KYR_s e^{KXR_s})}{KR_s} \quad (2)$$

$$\text{with } X = \frac{I_L + I_0 - \frac{V}{R_p}}{(1 + \frac{R_s}{R_p})}, Y = \frac{I_0 e^{KV}}{(1 + \frac{R_s}{R_p})} \text{ and } K = \frac{q}{AKT}$$

Next, we have the bypass diode which will be modeled using the simplified version of the Shockley diode equation (3).

$$I_b = I_r e^{\frac{-qV}{NkT}} \quad (3)$$

The parameters and their description as well as values used for the later simulations are detailed in Table 1. Combining the PV module current with the bypass diode current gives us total current output of each one of these PV + bypass diode block (4).

$$I_{total} = X - \frac{\text{Lambert}(KYR_s e^{KXR_s})}{KR_s} + I_r e^{\frac{-qV}{NkT}} \quad (4)$$

Since these blocks of PV + bypass are connected in series, it means that their combined voltage output equals the sum of their respective voltage when operating under the same current. For this reason, we need to interpolate the above obtained $I = f(V, G, T)$ into $V = g(I, G, T)$, so that we can add the voltage of each block for a given current. An

illustration of the method is given in Figure 4. This work can be done using MATLAB via the function 'interp1()'.

Table 1 Parameter description and numerical values of the PV module and bypass diodes used

Name	Description	Value	Unit
G	PV module irradiation	Variable	Wm^{-2}
G_{ref}	Standard irradiation	1000	Wm^{-2}
T	PV module temperature	Variable	K
T_{ref}	Reference temperature	298.15	K
V_{ocn}	Open circuit voltage	3.8	V
I_{scn}	Short circuit current	1	A
R_s	Equivalent serial resistance of PV module	0.2	Ω
R_p	Equivalent parallel resistance of PV module	1200	Ω
k_v	Voltage temperature coefficient	-0.0026	VK^{-1}
k_i	Current temperature coefficient	0.0023	AK^{-1}
A	PV module equivalent diode ideality factor	9.5	
q	Electron charge	1.6×10^{-19}	C
k	Boltzmann constant	1.38×10^{-23}	JK^{-1}
I_r	Bypass diode reverse saturation current	0.017	A
N	Bypass diode ideality factor	4.23	

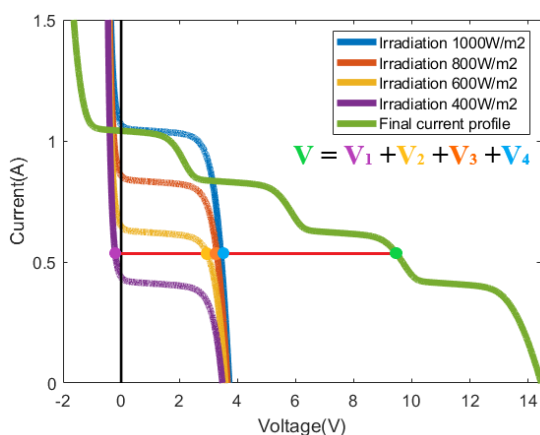


Figure 4 Illustration of how to obtain the current output of the array of 4 PV modules + bypass diodes

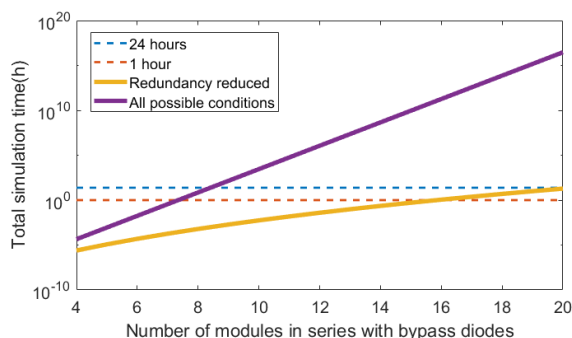


Figure 5 Time estimation to complete the sweep of 20 irradiation level per module for N modules in series

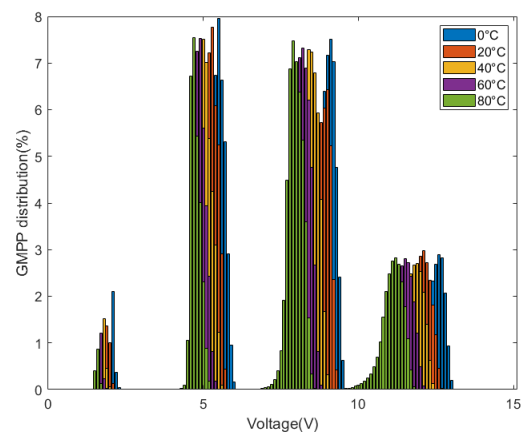


Figure 6 GMPP probability distribution of PV array consisting of 4 modules in series with 4 bypass diodes (equal probability supposed)

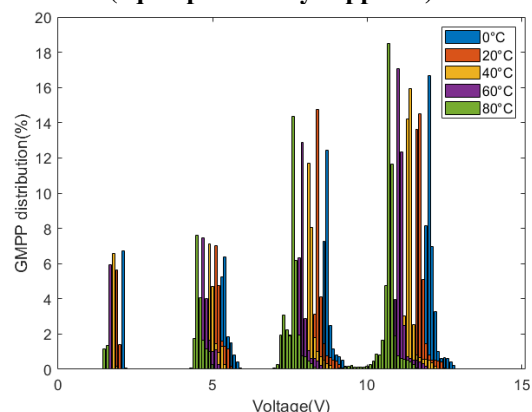


Figure 7 GMPP probability distribution of PV array consisting of 4 modules in series with 4 bypass diodes (real irradiation measurements)

3. GMPP distribution of the PV array

Using the previously described method, we can vary the irradiation for each module from 0 to 1000 Wm^{-2} in steps of 10 Wm^{-2} , find the GMPP and register the voltage where GMPP occurred. To further improve its predicting capabilities, we also vary the temperature from 0°C to 80°C in steps of 20°C , supposing homogenous temperatures for all modules, which should cover a wider operating range. The result obtained is presented in **Figure 6**. It confirms that for a given temperature, the GMPP can be found in clear clusters on the voltage range and consistent with the approximation that it should falls in the vicinity of $0.8V_{\text{ocn}}$ plus some multiples of V_{ocn} , sans some voltage drop caused by activated bypass diodes. We can also observe that for increasing temperature, the peak distribution shifts toward the left (lower voltage) which is consistent with the negative voltage coefficient of monocrystalline silicon. Another distribution result based on real world irradiation measurement can be found in **Figure 7**, acquired using 4 SP Lite2 pyranometers strapped to the back of a bicycle during a ride of around 1 hour around Toulouse, France (10h34 to 11h22, 21/06/2021). The sampling frequency is 5kHz per channel with subsequent filtering making the effective sampling frequency 100Hz. The resulting graph was also filtered of power peaks below 1W because they are not realistically extractable.

However, we should also note about several optimization taken during this step to avoid excessive runtimes. The first problem is with ‘interp1()’ function which is computationally intensive comparing to other vector operations and should be done only once. Therefore, the program calculates the I/V profile of the PV module + bypass for all irradiation and temperatures only once and store these I/V into memory. To construct the overall, I/V of the entire array, a simple addition is necessary which drastically reduces runtime (about a factor of 1000) (Table 2).

Table 2 Average execution time of each iteration in the loop for 3 different simulation methods

Method	Time (μs)
Simulink	672000
‘interp1() at each iteration’	8000
Precalculated table	9

The second optimization is the removal of redundant conditions. For an array of PV modules in series, whether they receive 1000-800-400-200Wm⁻² respectively or 1000-400-800-200Wm⁻² respectively should give the same output. The time gained from this can be observed in Figure 5, plotting the amount of time needed to sweep an array of N modules in series with a precision of 20 levels of irradiation per module. By choosing the arbitrary limit of simulation time to 1 day, we see that instead being capable of checking only 8 modules in series without optimization, we can check up to 20 modules in series. This means that the presented method can be scaled up to more powerful systems beyond 100W.

4. Proposed improved P&O fast GMPPT

With the distribution graph clearly denominating zones where the GMPP can be found, we can conclude that randomly searching the voltage range, or calculating the power at each iteration is not necessary. Instead, we propose a fast GMPPT method where we only measure the power at 3 specific voltage values and continue with P&O where the power obtained is the highest. To evaluate the feasibility of such algorithm, we devise the following criteria (Figure 8):

- If the power gradient from the chosen voltage point and the GMPP is constantly increasing, it means that a P&O from that point can reach GMPP.
- Otherwise, P&O will be stuck in a local peak and fail to reach GMPP.

By choosing 3 voltage values 5.2V, 8.2V and 12.2V on the sweep performed in Figure 6, and by applying the aforementioned criteria to evaluate the probability of finding GMPP, we have a success rate of 93.64% over 22106375 distinct irradiation/temperature conditions checked, 3.46% failure rate and 2.89% are power at GMPP too low to be extractable (i.e. below 1W) or inaccessible peaks. This is because we will be testing this method on a buck converter that output to a Li-ion battery operating at around 3.2-4V.

Moving on to the implementation on a buck converter, reaching only 3 voltage points is not a trivial task because

there is no linear relationship between the duty cycle and input voltage, but we can regulate the duty cycle so that the input voltage approaches the desired values. Given that during this regulation only a comparison needs to be made (whether voltage measured equals what we want), the algorithm still retains its simplicity. Furthermore, by registering the duty cycles that correspond to each one of the desired voltage points during the last search, subsequent scans should take considerably less time to finish than the initial initialization.

For the converter, we use a DC/DC buck converter whose averaged model can be found in Figure 9. For the preliminary evaluation of our proposed method, we are going to compare it against P&O [4], deterministic PSO (DPSO) [40], GWO [20] and ABC [18]. All algorithms are written in our application context using the description from their respective articles. Since the converter’s response time to any duty cycle step is at most 3ms, the commands will be sent at 5ms intervals. The test conditions would be for 3 irradiation conditions in Figure 1, initially starting at condition (1), changing to (2) and then to (3). Temperature is fixed for all modules at 60°C. For condition (1) where the array is evenly irradiated (Figure 10), P&O converged rapidly and without oscillation thanks to its optimal starting position, then we have GWO and DPSO converges relatively quickly around 80ms, our method converges a bit slower at around 120ms and finally ABC converges late at around 170ms. Concerning the amount of power obtained, there is no clear edge for any of the methods. When the condition changes from (1) to (2) (Figure 11), the GMPP position changes rapidly from around 12V down to 5V with a local peak around 9V, and it is here that P&O shows its weakness, with GWO also failing to converge toward global peak, however this seems to vary from run to run. Our proposed method converges around 20ms later than DPSO at around 90ms with ABC the last to converge toward global peak. Finally, when the condition changes from (2) to (3) (Figure 12), the GMPP changes to around 9V and here we have P&O, our method, DPSO and GWO all converges at around the same speed, with ABC again trailing behind. We also observe the effects of memorization of the previous duty cycles on the voltage search phase: 8 steps, then 7 steps then 5 steps.

With this result, our method is not strictly superior in terms of convergence time, nor does it guarantee that the system will arrive at GMPP all the time. However, in terms of implementation complexity, the most complex operation is integer multiplication to obtain the power values, which is on par with P&O. This is also true for DPSO, however it has more comparisons and multiplications at each control cycle. Finally, we have GWO and ABC integrating a lot of randomized numbers, floating point multiplications and divisions.



Figure 8 Illustration of success and failure criteria for propose fast GMPPT method

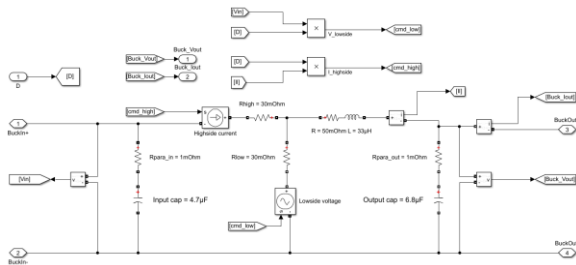


Figure 9 Averaged DC/DC buck converter model used for the Simulink model

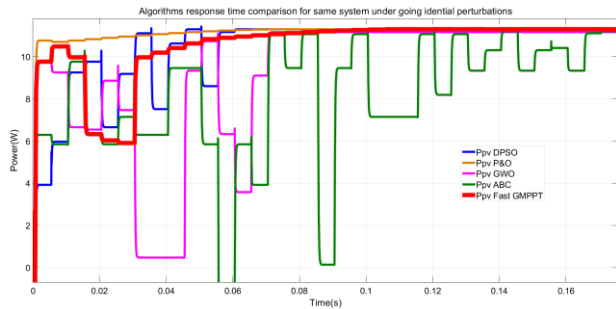


Figure 10 Algorithms comparison, condition (1): 1000 - 1000 - 1000 - 1000Wm⁻²

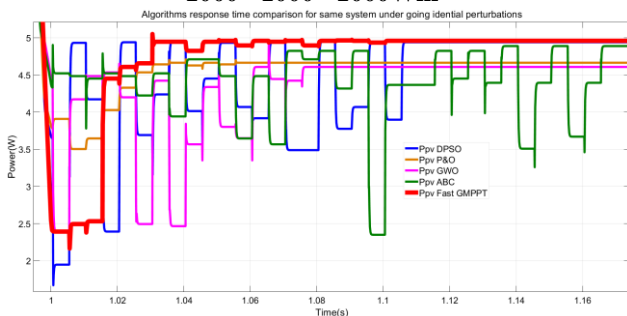


Figure 11 Algorithms comparison, condition (2): 1000 - 1000 - 500 - 200Wm⁻²

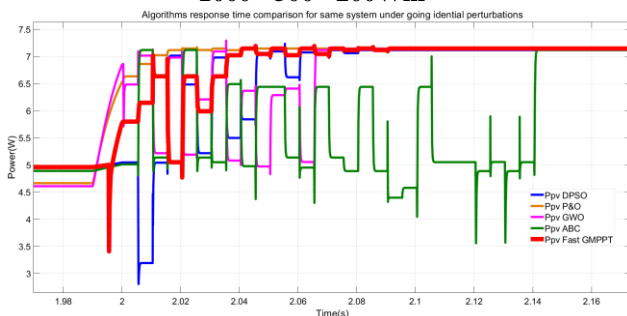


Figure 12 Algorithms comparison, condition (3): 1000 - 1000 - 800 - 500Wm⁻²

5. Conclusions

In this paper, an efficient method to quickly simulate the power output of an array under a large amount of weather conditions was presented together with optimizations that made it possible. Using this capability, we plotted the distribution of the GMPP on the voltage range proving clear zone delineation for this application of 4 PV modules with 4 bypass diodes and estimated that our proposed fast-tracking method can reach GMPP in 93.64% of the time. The Simulink simulation result compared versus other lightweight algorithms like DPSO, P&O, GWO, ABC

shows promise and warrants further research with testing on real hardware as well as real world weather conditions.

References

- [1] K. A. Kim and P. T. Krein, "Photovoltaic hot spot analysis for cells with various reverse-bias characteristics through electrical and thermal simulation," in *2013 IEEE 14th Workshop on Control and Modeling for Power Electronics (COMPEL)*, Jun. 2013, pp. 1–8. doi: 10.1109/COMPEL.2013.6626399.
- [2] H. Mohammed, M. Kumar, and R. Gupta, "Bypass diode effect on temperature distribution in crystalline silicon photovoltaic module under partial shading," *Sol. Energy*, vol. 208, pp. 182–194, Sep. 2020, doi: 10.1016/j.solener.2020.07.087.
- [3] J. C. Teo, R. Tan, V. H. Mok, V. Ramachandaramurthy, and C. Tan, "Impact of Partial Shading on the P-V Characteristics and the Maximum Power of a Photovoltaic String," *Energies*, 2018, doi: 10.3390/EN11071860.
- [4] M. A. G. de Brito, L. Galotto, L. P. Sampaio, G. de A. e Melo, and C. A. Canesin, "Evaluation of the Main MPPT Techniques for Photovoltaic Applications," *IEEE Trans. Ind. Electron.*, vol. 60, no. 3, pp. 1156–1167, Mar. 2013, doi: 10.1109/TIE.2012.2198036.
- [5] E. Koutroulis, K. Kalaitzakis, and N. C. Voulgaris, "Development of a microcontroller-based, photovoltaic maximum power point tracking control system," *IEEE Trans. Power Electron.*, vol. 16, no. 1, pp. 46–54, Jan. 2001, doi: 10.1109/63.903988.
- [6] S. Jain and V. Agarwal, "A new algorithm for rapid tracking of approximate maximum power point in photovoltaic systems," *IEEE Power Electron. Lett.*, vol. 2, no. 1, pp. 16–19, Mar. 2004, doi: 10.1109/LPEL.2004.828444.
- [7] W. Li, Y. Zheng, W. Li, Y. Zhao, and X. He, "A smart and simple PV charger for portable applications," in *2010 Twenty-Fifth Annual IEEE Applied Power Electronics Conference and Exposition (APEC)*, Feb. 2010, pp. 2080–2084. doi: 10.1109/APEC.2010.5433522.
- [8] V. V. R. Scarpa, S. Buso, and G. Spiazzi, "Low-Complexity MPPT Technique Exploiting the PV Module MPP Locus Characterization," *IEEE Trans. Ind. Electron.*, vol. 56, no. 5, pp. 1531–1538, May 2009, doi: 10.1109/TIE.2008.2009618.
- [9] R. F. Coelho, F. M. Concer, and D. C. Martins, "A MPPT approach based on temperature measurements applied in PV systems," in *2010 IEEE International Conference on Sustainable Energy Technologies (ICSET)*, Dec. 2010, pp. 1–6. doi: 10.1109/ICSET.2010.5684440.
- [10] W.-M. Lin, C.-M. Hong, and C.-H. Chen, "Neural-Network-Based MPPT Control of a Stand-Alone Hybrid Power Generation System," *IEEE Trans. Power Electron.*, vol. 26, no. 12, pp. 3571–3581, Dec. 2011, doi: 10.1109/TPEL.2011.2161775.
- [11] A. Ramyar, H. Iman-Eini, and S. Farhangi, "Global Maximum Power Point Tracking Method for Photovoltaic Arrays Under Partial Shading Conditions," *IEEE Trans. Ind. Electron.*, vol. 64, no. 4, pp. 2855–2864, Apr. 2017, doi: 10.1109/TIE.2016.2632679.
- [12] B. Veerasamy, A. R. Thelkar, G. Ramu, and T. Takeshita, "Efficient MPPT control for fast irradiation changes and partial shading conditions on PV systems," in *2016 IEEE International Conference on Renewable Energy Research and Applications (ICRERA)*, Nov. 2016, pp. 358–363. doi: 10.1109/ICRERA.2016.7884360.
- [13] J. Ahmad, F. Spertino, P. Di Leo, and A. Ciocia, "A Variable Step Size Perturb and Observe Method Based MPPT for Partially Shaded Photovoltaic Arrays," in *PCIM Europe 2016; International Exhibition and Conference for Power Electronics, Intelligent Motion, Renewable Energy and Energy Management*, May 2016, pp. 1–8.
- [14] N. Priyadarshi, A. Anand, A. Sharma, F. Azam, V. Singh, and R. Sinha, "An Experimental Implementation and Testing of GA based Maximum Power Point Tracking for PV System under Varying Ambient Conditions Using dSPACE DS 1104 Controller," *Int. J. Renew. Energy Res. IJRES*, vol. 7, no. 1, Art. no. 1, Mar. 2017.
- [15] K. S. Tey, S. Mekhilef, H.-T. Yang, and M.-K. Chuang, "A Differential Evolution Based MPPT Method for Photovoltaic Modules

- under Partial Shading Conditions,” *Int. J. Photoenergy*, vol. 2014, p. e945906, May 2014, doi: 10.1155/2014/945906.
- [16] S. Roy Chowdhury and H. Saha, “Maximum Power Point Tracking of Partially Shaded Solar Photovoltaic Arrays,” *Sol. Energy Mater. Sol. Cells - Sol. ENERGMATER Sol. CELLS*, vol. 94, pp. 1441–1447, Sep. 2010, doi: 10.1016/j.solmat.2010.04.011.
- [17] M. Miyatake, M. Veerachary, F. Toriumi, N. Fujii, and H. Ko, “Maximum Power Point Tracking of Multiple Photovoltaic Arrays: A PSO Approach,” *IEEE Trans. Aerosp. Electron. Syst.*, vol. 47, no. 1, pp. 367–380, Jan. 2011, doi: 10.1109/TAES.2011.5705681.
- [18] D. Pilakkat and S. Kanthalakshmi, “An improved P&O algorithm integrated with artificial bee colony for photovoltaic systems under partial shading conditions,” *Sol. Energy*, vol. 178, pp. 37–47, Jan. 2019, doi: 10.1016/j.solener.2018.12.008.
- [19] R. Sridhar, C. Subramani, and S. Pathy, “A grasshopper optimization algorithm aided maximum power point tracking for partially shaded photovoltaic systems,” *Comput. Electr. Eng.*, vol. 92, p. 107124, Jun. 2021, doi: 10.1016/j.compeleceng.2021.107124.
- [20] S. K. Cherukuri and S. R. Rayapudi, “Enhanced Grey Wolf Optimizer Based MPPT Algorithm of PV System Under Partial Shaded Condition,” *Int. J. Renew. Energy Dev.*, vol. 6, no. 3, pp. 203–212, Nov. 2017, doi: 10.14710/ijred.6.3.203-212.
- [21] S. Mohanty, B. Subudhi, and P. K. Ray, “A New MPPT Design Using Grey Wolf Optimization Technique for Photovoltaic System Under Partial Shading Conditions,” *IEEE Trans. Sustain. Energy*, vol. 7, no. 1, pp. 181–188, Jan. 2016, doi: 10.1109/TSTE.2015.2482120.
- [22] S. Mohanty, B. Subudhi, and P. K. Ray, “A Grey Wolf-Assisted Perturb & Observe MPPT Algorithm for a PV System,” *IEEE Trans. Energy Convers.*, vol. 32, no. 1, pp. 340–347, Mar. 2017, doi: 10.1109/TEC.2016.2633722.
- [23] J. Prasanth Ram and N. Rajasekar, “A Novel Flower Pollination Based Global Maximum Power Point Method for Solar Maximum Power Point Tracking,” *IEEE Trans. Power Electron.*, vol. 32, no. 11, pp. 8486–8499, Nov. 2017, doi: 10.1109/TPEL.2016.2645449.
- [24] R. S. Pal and V. Mukherjee, “A novel population based maximum point tracking algorithm to overcome partial shading issues in solar photovoltaic technology,” *Energy Convers. Manag.*, vol. 244, p. 114470, Sep. 2021, doi: 10.1016/j.enconman.2021.114470.
- [25] E. Lodhi *et al.*, “Dragonfly Optimization-based MPPT Algorithm for Standalone PV System under Partial Shading,” in *2021 IEEE International Conference on Emergency Science and Information Technology (ICESIT)*, Nov. 2021, pp. 277–283. doi: 10.1109/ICESIT53460.2021.9697000.
- [26] S. Titri, C. Larbes, K. Y. Toumi, and K. Benatchba, “A new MPPT controller based on the Ant colony optimization algorithm for Photovoltaic systems under partial shading conditions,” *Appl. Soft Comput.*, vol. 58, pp. 465–479, Sep. 2017, doi: 10.1016/j.asoc.2017.05.017.
- [27] A. F. Mirza, M. Mansoor, and Q. Ling, “A novel MPPT technique based on Henry gas solubility optimization,” *Energy Convers. Manag.*, vol. 225, p. 113409, Dec. 2020, doi: 10.1016/j.enconman.2020.113409.
- [28] J. Ahmed and Z. Salam, “A Maximum Power Point Tracking (MPPT) for PV system using Cuckoo Search with partial shading capability,” *Appl. Energy*, vol. 119, pp. 118–130, Apr. 2014, doi: 10.1016/j.apenergy.2013.12.062.
- [29] B. N. Alajmi, K. H. Ahmed, S. J. Finney, and B. W. Williams, “Fuzzy-Logic-Control Approach of a Modified Hill-Climbing Method for Maximum Power Point in Microgrid Standalone Photovoltaic System,” *IEEE Trans. Power Electron.*, vol. 26, no. 4, pp. 1022–1030, Apr. 2011, doi: 10.1109/TPEL.2010.2090903.
- [30] R. Kumar, B. Kumar, and S. D., “Fuzzy Logic based Improved P&O MPPT Technique for Partial Shading Conditions,” in *2018 International Conference on Computing, Power and Communication Technologies (GUCON)*, Sep. 2018, pp. 775–779. doi: 10.1109/GUCON.2018.8674917.
- [31] U. Yilmaz, A. Kircay, and S. Borekci, “PV system fuzzy logic MPPT method and PI control as a charge controller,” *Renew. Sustain. Energy Rev.*, vol. 81, pp. 994–1001, Jan. 2018, doi: 10.1016/j.rser.2017.08.048.
- [32] Md. M. Rahman and M. S. Islam, “Artificial Neural Network Based Maximum Power Point Tracking of a Photovoltaic System,” in *2019 3rd International Conference on Electrical, Computer Telecommunication Engineering (ICECTE)*, Dec. 2019, pp. 117–120. doi: 10.1109/ICECTE48615.2019.9303531.
- [33] D. T. Coffas, P. A. Coffas, and S. Kaplanis, “Methods to determine the dc parameters of solar cells: A critical review,” *Renew. Sustain. Energy Rev.*, vol. 28, pp. 588–596, Dec. 2013, doi: 10.1016/j.rser.2013.08.017.
- [34] M. G. Villalva, J. R. Gazoli, and E. R. Filho, “Comprehensive Approach to Modeling and Simulation of Photovoltaic Arrays,” *IEEE Trans. Power Electron.*, vol. 24, no. 5, pp. 1198–1208, May 2009, doi: 10.1109/TPEL.2009.2013862.
- [35] K. Ding, J. Zhang, X. Bian, and J. Xu, “A simplified model for photovoltaic modules based on improved translation equations,” *Sol. Energy*, vol. 101, pp. 40–52, Mar. 2014, doi: 10.1016/j.solener.2013.12.016.
- [36] X. H. Nguyen and M. P. Nguyen, “Mathematical modeling of photovoltaic cell/module/arrays with tags in Matlab/Simulink,” *Environ. Syst. Res.*, vol. 4, no. 1, p. 24, Dec. 2015, doi: 10.1186/s40068-015-0047-9.
- [37] E. Roibás-Millán *et al.*, “Lambert W-function simplified expressions for photovoltaic current-voltage modelling,” in *2020 IEEE International Conference on Environment and Electrical Engineering and 2020 IEEE Industrial and Commercial Power Systems Europe (EEEIC / I CPS Europe)*, Jun. 2020, pp. 1–6. doi: 10.1109/EEEIC/ICPSEurope49358.2020.9160734.
- [38] E. Batzelis, G. Anagnostou, C. Chakraborty, and B. C. Pal, “Computation of the Lambert W function in photovoltaic modeling,” presented at the ELECTRIMACS 2019, May 2019.
- [39] P. Upadhyay, S. Pulipaka, R. Kumar, and M. Sharma, “Parameter extraction of solar photovoltaic system using Lambert-W function for different environmental condition,” in *2016 IEEE Region 10 Conference (TENCON)*, Nov. 2016, pp. 1884–1888. doi: 10.1109/TENCON.2016.7848349.
- [40] K. Ishaque and Z. Salam, “A Deterministic Particle Swarm Optimization Maximum Power Point Tracker for Photovoltaic System Under Partial Shading Condition,” *IEEE Trans. Ind. Electron.*, vol. 60, no. 8, pp. 3195–3206, Aug. 2013, doi: 10.1109/TIE.2012.2200223.